Compton Scattering Experiments with Polychromatic Radiation *

Wolfgang Schütz, Beate Waldeck, Dietmar Flösch, and Wolf Weyrich
Fakultät für Chemie, Universität Konstanz, Konstanz, Federal Republic of Germany

Z. Naturforsch. **48a**, 352–357 (1993); reveived January 26, 1993

We show an iterative algorithm that allows to obtain accurate Compton profiles $J(q)$ from Compton scattering spectra $I_2(\omega_2)$, if the excitation radiation is not strictly monochromatic. It requires knowledge of the spectral distribution of the primary radiation $I_1(\omega_1)$, validity of the impulse approximation and dominance of a monochromatic part in $I_1(\omega_1)$ over the polychromatic rest. Conversely, the primary spectrum is often experimentally not directly accessible. In such a situation it is possible to evaluate the primary spectrum $I_1(\omega_1)$ from the spectrum of scattered photons, $I_2(\omega_2)$, with a similar iterative algorithm. We use a scattering target of high atomic number in order to ensure that the elastically scattered photons dominate the inelastically scattered ones. From the scattered spectrum we get a model for the Compton profile that allows us to separate the inelastic part of the scattered spectrum from the elastic part, which, in turn, is proportional to the spectral distribution of the primary radiation.

Key words: Compton spectroscopy, Polychromaticity, Scattering cross-section.

1. Introduction

Compton spectroscopy has become a well-established tool for the direct investigation of projections of the electron momentum density [1, 2] and therefore of the electronic structure of the chemical bond. Long-range (> 5 Å) intermolecular interactions can only be examined if the momentum resolution is better than $\approx 0.2\, p_0$ ($p_0 = \hbar/a_0 = 1$ Dumond $= 1.99289 \cdot 10^{-24}$ kg m/s). This can only be achieved with crystal analysers. The reflectivity of such crystals is very low, whence sources of higher intensity are required. Synchrotron radiation has been used for some years with great success [3, 4]. With conventional, much cheaper and continuously available sources, on the other hand, higher intensity is attained only at the expense of a lower degree of monochromatisation. Strong γ-ray sources have a low-energy tail owing to internal inelastic scattering with an integral intensity of up to several percent of the main peak [5]. Manninen et al. [6] and Rollason et al. [7] discussed this problem in detail. Imperfect monochromatisation of an X-ray tube is another example.

In the scope of the impulse approximation, the Compton profile (i.e. the projection of the momentum density along the scattering vector) is directly proportional to the scattering spectrum. This, however, is valid only if ideal monochromatic excitation radiation can be assumed. In Sect. 2 we show an iterative algorithm that enables us to obtain the accurate Compton profile also in those cases where the assumption of monochromatic excitation is not valid. The algorithm is applicable if the spectral distribution of the exciting radiation – the primary spectrum – is known and if it can be subdivided into a dominating monochromatic part and a polychromatic remainder. Our procedure applies not only to low-energy tails of γ-ray sources but to all possible spectral shapes of polychromaticity.

In some experimental cases, however, the true primary spectrum is not directly accessible, e.g. because the radiation is too intense to be measured by an energy discriminating detector. We show in Sect. 3 that it is possible to obtain the intensity distribution of the primary spectrum from a scattered spectrum by a similar iterative algorithm. In that case we use a scattering target of high atomic number to ensure that the elastically scattered photons dominate the inelastically scattered ones. From the scattered spectrum we obtain a model for the Compton profile by a nonlinear least-squares fitting procedure that allows us to separate the inelastic part of the scattered spectrum from the elastic part, which is proportional to the primary spectrum.

* Presented at the Sagamore X Conference on Charge, Spin and Momentum Densities, Konstanz, Fed. Rep. of Germany, September 1–7, 1991.

Reprint requests to Prof. Dr. Dr. h.c. Wolf Weyrich, Lehrstuhl für Physikalische Chemie I, Fakultät für Chemie, Universität Konstanz, Postfach 55 60, D-W-7750 Konstanz, Fed. Rep. of Germany.

0932-0784 / 93 / 0100-0352 $ 01.30/0. – Please order a reprint rather than making your own copy.

2. Accurate Compton Profiles

For a given scattering cross-section model, the evaluation of Compton profiles $J(q)$ is straightforward, if strict monochromaticity of the primary radiation is assumed and if $J(q)$ is a multiplicative part of the cross-section [8]. In most experimental cases monochromaticity is not guaranteed. We here present an algorithm that allows us to obtain the accurate Compton profile also in those cases, provided the spectral distribution of the primary radiation $I_1(\omega_1)$ is known*.

The scattering spectrum $I_2(\omega_2)$ is a function of the primary spectrum $I_1(\omega_1)$ and the scattering power $Q(\omega_1, \omega_2, \varphi)$ of the target; owing to the different final states, $I_2(\omega_2)$ can be subdivided into an elastic and an inelastic part:

$$I_2(\omega_2) = \int I_1(\omega_2)\, Q(\omega_1, \omega_2, \varphi)\, \mathrm{d}\omega_1 \tag{1}$$
$$= I_1(\omega_2) Q_0(\omega_1, \varphi) + \int I_1(\omega_1)\, A(\omega_1, \omega_2, \varphi) \cdot C(\omega_1, \omega_2, \varphi)\, J(q)\, \mathrm{d}\omega_1 .$$

$Q_0(\omega_2, \varphi)$ is porportional to the Thomson scattering cross-section, $A(\omega_1, \omega_2, \varphi)$ the absorption factor and $C(\omega_1, \omega_2, \varphi) \cdot J(q)$ a cross-section model containing $J(q)$ multiplicatively. The momentum component q is a function of both ω_1 and ω_2 (and, of course, of the scattering angle φ, which is a constant parameter of the traditional isogonal experiment).

* We use $\hbar = 1$ throughout the paper.

Therefore, the first correction is to eliminate the elastically scattered part of $I_2(\omega_2)$ by subtracting the correctly weighted $I_1(\omega_2)$:

$$I_{2,\mathrm{inel}}(\omega_2) = I_2(\omega_2) - I_1(\omega_2) Q_0(\omega_2, \varphi) \tag{2}$$
$$= \int I_1(\omega_1)\, A(\omega_1, \omega_2, \varphi)\, C(\omega_1, \omega_2, \varphi)\, J(q)\, \mathrm{d}\omega_1 .$$

This correction is necessary especially when targets of high atomic number are investigated. In practice the correction factor is given by the ratio of the dominating Rayleigh peak in the scattering spectrum to the same peak in the primary spectrum.

Now the crucial point is the subdivision of the primary spectrum into a dominating monochromatic part of energy $\omega_{1,\mathrm{m}}$ and a polychromatic remainder,

$$I_1(\omega_1) = I^0_{1,\mathrm{m}}\, \delta(\omega_1 - \omega_{1,\mathrm{m}}) + I_{1,\mathrm{p}}(\omega_1) , \tag{3}$$

which by insertion in (2) leads to

$$I_{2,\mathrm{inel}}(\omega_2) = I^0_{1,\mathrm{m}}\, C(\omega_{1,\mathrm{m}}, \omega_2, \varphi)\, A(\omega_{1,\mathrm{m}}, \omega_2, \varphi)\, J(q_\mathrm{m}) + \int I_{1,\mathrm{p}}(\omega_1)\, A(\omega_1, \omega_2, \varphi)\, C(\omega_1, \omega_2, \varphi)\, J(q)\, \mathrm{d}\omega_1 \tag{4}$$

with q_m being the momentum component calculated from $\omega_{1,\mathrm{m}}$ and ω_2. This can be solved for $J(q_\mathrm{m})$,

$$J(q_\mathrm{m}) = \frac{I_{2,\mathrm{m}}(\omega_2) - \int I_{1,\mathrm{p}}(\omega_1)\, A(\omega_1, \omega_2, \varphi)\, C(\omega_1, \omega_2, \varphi)\, J(q)\, \mathrm{d}\omega_1}{I_{1,\mathrm{m}}\, A(\omega_{1,\mathrm{m}}, \omega_2, \varphi)\, C(\omega_{1,\mathrm{m}}, \omega_2, \varphi)} , \tag{5}$$

which can be interpreted as an iteration scheme for the determination of the true Compton profile. The zeroth approximation is obtained by neglecting the polychromatic part. Each improvement is calculated by subtracting the polychromatic contributions on the basis of the $J(q)$ obtained up to then:

$$J^{(0)}(q_\mathrm{m}) = \frac{I_{2,\mathrm{inel}}(\omega_2)}{I_{1,\mathrm{m}}\, A(\omega_{1,\mathrm{m}}, \omega_2, \varphi)\, C(\omega_{1,\mathrm{m}}, \omega_2, \varphi)} ,$$

$$J^{(i+1)}(q_\mathrm{m}) = \frac{I_{2,\mathrm{inel}}(\omega_2) - \int I_{1,\mathrm{p}}(\omega_1)\, A(\omega_1, \omega_2, \varphi)\, C(\omega_1, \omega_2, \varphi)\, J^{(i)}(q)\, \mathrm{d}\omega_1}{I_{1,\mathrm{m}} A(\omega_{1,\mathrm{m}}, \omega_2, \varphi)\, C(\omega_{1,\mathrm{m}}, \omega_2, \varphi)} . \tag{6}$$

This procedure is repeated until self-consistency of $J(q)$ is achieved.

The experiment yields the spectra as vectors of discrete data points, and therefore the integral becomes a sum. The correction of the $J(q)$ is best carried out from the high-energy end downwards, since there is no anti-Stokes part with $\omega_2 > \omega_1$ in the Compton spectra of targets in the electronic ground state. Thus the $J(q)$ vector is improved continuously even *within* each iteration cycle, similar to the tail-stripping in the processing of high-energy γ-ray spectra. This "stripping" strategy contributes significantly to the fast convergence.

The algorithm was implemented as a FORTRAN-77 program under the operating system VMS. It has been

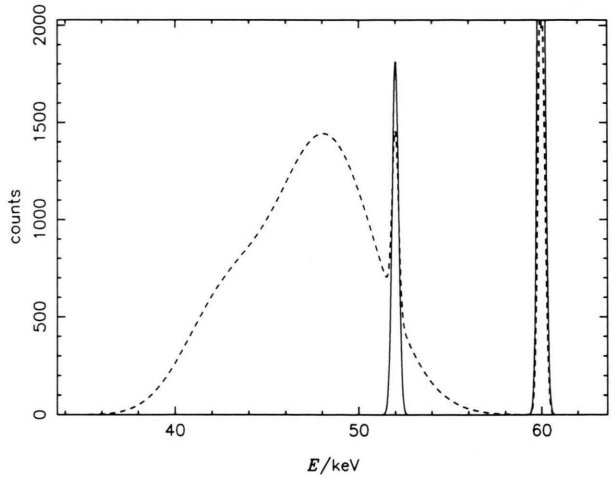

Fig. 1 a. "Synthetic" primary spectrum consisting of a dominating peak at 60 keV and a second line at 52 keV of 40% intensity (solid line), and the resulting scattering spectrum, calculated on the basis of a Gaussian shaped Compton profile (dashed line).

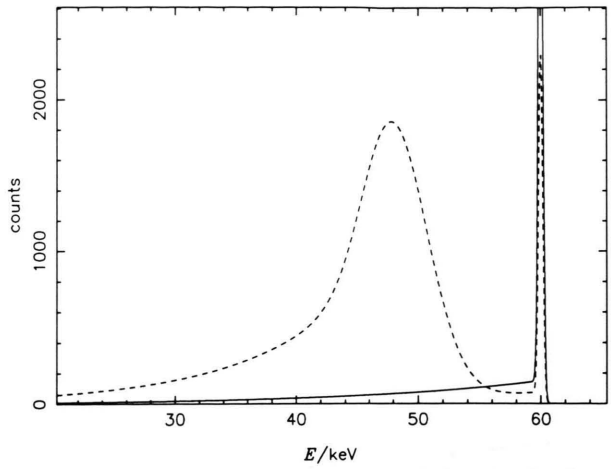

Fig. 2 a. "Synthetic" primary spectrum consisting of a dominating peak at 60 keV and a low-energy tail of ≈ 40% intensity (solid line) and the resulting scattering spectrum, calculated on the basis of a Gaussian shaped Compton profile (dashed line).

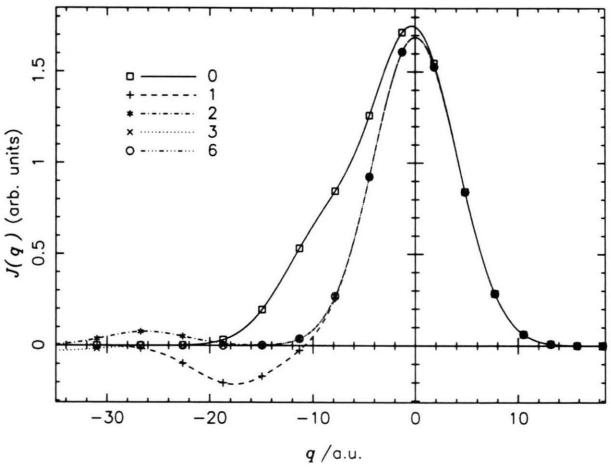

Fig. 1 b. The resulting Compton profile at different stages of the iteration: 0th approximation (□), result of 1st (+), 2nd (∗) and 3rd (×) cycle, final result (○).

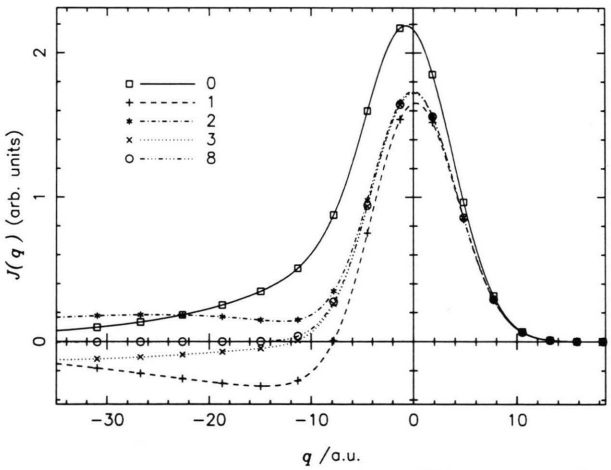

Fig. 2 b. The resulting Compton profile at different stages of the iteration: 0th approximation (□), result of 1st (+), 2nd (∗) and 3rd (×) cycle, final result (○).

tested by the following procedure. Starting from a Gaussian-shaped model Compton-profile $J(q) \propto \exp(-0.03\, q^2)$ and a given primary spectrum, we calculated the resulting scattering spectrum on the basis of a particular scattering cross-section. We chose the model of Ribberfors [9] with some slight simplifications. Both spectra were convoluted with a realistic resolution function.

Figure 1 a shows a "synthetic" primary spectrum consisting of a dominating peak at 60 keV and a second line at 52 keV (40% intensity) together with the corresponding scattering spectrum. In Fig. 1 b the resulting Compton profile is shown at different stages of the iteration. One clearly sees the over-correction on the low-momentum side of the Compton profile in the first step of the iteration, because the $J(q)$ determined in the zeroth approximation is strongly asymmetric. An alternating sequence of $J^{(i)}(q)$ follows, which, however, converges rapidly. After five iteration cycles there is no significant change left. The obtained

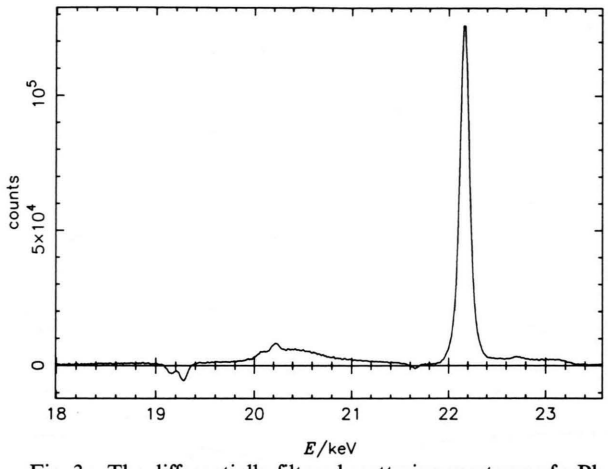

Fig. 3a. The differentially-filtered scattering spectrum of a Pb target with a dominating Rayleigh peak from the $AgK\alpha_1$ line, a broad Compton band mainly caused by the $AgK\alpha_1$ radiation, fluorescence lines of the filter materials Ru (negative) and Rh, and a rest of the bremsstrahlung background.

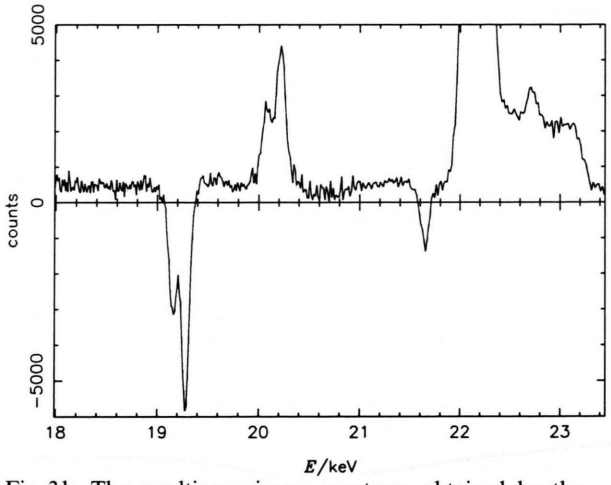

Fig. 3b. The resulting primary spectrum obtained by the simple iteration scheme.

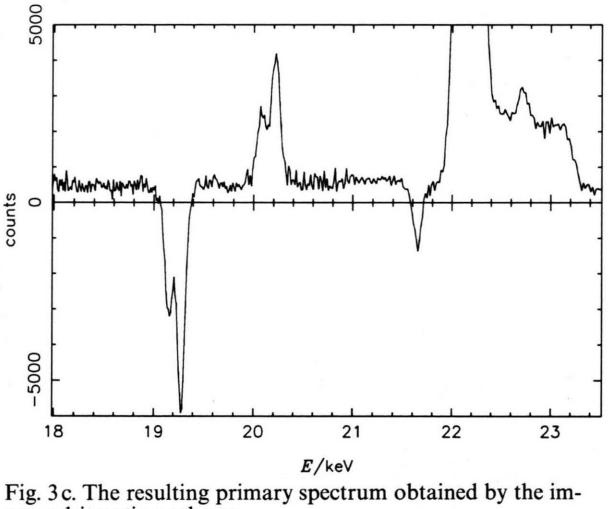

Fig. 3c. The resulting primary spectrum obtained by the improved iteration scheme.

Compton profile is the same as the original Gaussian-shaped one within full numerical accuracy. Figures 2a and b show the same results for a primary spectrum consisting of a single line with an exponential low-energy tail of $\approx 40\%$ integral intensity. In comparison to the 6–10% tail of a ^{241}Am γ-ray source [5], this is a worst-case study that proves convergence also under unfavourable circumstances.

3. Determination of the Spectral Distribution of the Primary Radiation

Often, however, the primary spectrum $I_1(\omega_1)$ is not directly measurable. In this section we present a related algorithm that allows us to obtain $I_1(\omega_1)$ from the scattering spectrum of a target of high atomic number. In such a case the scattering spectrum is dominated by the elastic part and is therefore nearly proportional to $I_1(\omega_1)$. The inelastically scattered part of the spectrum, however, must be separated.

In the following we shall demonstrate the determination of the differentially filtered spectrum of a wide-focus X-ray tube with Ag anode from a scattering spectrum of a Pb target. This method of monochromatisation, which was introduced by Ross [10] and consists in forming the difference between a Ru-filtered and a Rh-filtered spectrum, enables us to separate the $AgK\alpha_1$ line out of the tube spectrum, because the RuK absorption edge lies between the $AgK\alpha_2$ and $K\alpha_1$ line. Figure 3a shows the scattering spectrum with a dominating Rayleigh peak from the $AgK\alpha_1$ line, a broad Compton band mainly caused by the $AgK\alpha_1$ radiation, some fluorescence lines of the filter materials Ru (negative) and Rh, and a rest of the bremsstrahlung background (above $AgK\alpha_1$) owing to imperfect monochromatisation because of the 1.1 keV energy difference between the Ru and Rh absorption edges.

The elimination of the inelastically scattered part is based on a nonlinear least-squares fit of the scattering spectrum. We use Gaussian-type functions for the

Rayleigh and fluorescence peaks, a polynomial background and a sum of Lorentzian functions of higher degree for the Compton band:

$$I^{\mathrm{mod}}_{2,\,\mathrm{inel,\,m}}(\omega_2) = \sum_{i=1}^{n} I_{\mathrm{cp},\,i}\,\frac{\zeta_i^{2l_i}\,q_{\mathrm{m}}(\omega_2)^{k_i}}{[\zeta_i^2 + q_{\mathrm{m}}(\omega_2)^2]^{l_i}}\,. \tag{7}$$

$I_{\mathrm{cp},\,i}$ and ζ_i are the parameters optimised by the least-squares fit, q_{m} is the momentum component calculated from $\omega_{1,\,\mathrm{m}}$ and ω_2. This type of function is the Fourier transform of Slater-type functions [11] and therefore very suitable to fit the inelastic part of the spectrum. The subscript "m" indicates that the modelling was carried out under the assumption of perfect monochromaticity of the exciting primary radiation $I_1(\omega_1)$. Division by the scattering cross-section leads to a model for $J(q)$:

$$J^{\mathrm{mod}}(q) = \frac{I^{\mathrm{mod}}_{2,\,\mathrm{inel,\,m}}(\omega_2)}{I_{1,\,\mathrm{m}}\,A(\omega_{1,\,\mathrm{m}}, \omega_2, \varphi)\,C(\omega_{1,\,\mathrm{m}}, \omega_2, \varphi)}\,. \tag{8}$$

With this model we can eliminate the inelastically scattered part by the following iterative algorithm. Insertion of (8) in (1) leads to

$$I_1(\omega_2) \propto I_{2,\,\mathrm{el}}(\omega_2) = I_2(\omega_2) - \int I_1(\omega_1)\,A(\omega_1, \omega_2, \varphi) \cdot C(\omega_1, \omega_2, \varphi)\,J^{\mathrm{mod}}(q)\,\mathrm{d}\omega_1\,, \tag{9}$$

which is the iteration scheme for the determination of $I_1(\omega_1)$:

$$I_1^{(0)}(\omega_2) = I_2(\omega_2)\,, \tag{10}$$

$$I_1^{(i+1)}(\omega_2) = I_2(\omega_2) - \int I_1^{(i)}(\omega_1)\,A(\omega_1, \omega_2, \varphi) \cdot C(\omega_1, \omega_2, \varphi)\,J^{\mathrm{mod}}(q)\,\mathrm{d}\omega_1\,.$$

This procedure is repeated until self-consistency of $I_1(\omega_1)$ is achieved. Figure 3b shows the result of the iteration. One clearly sees that the inelastic contributions caused by the fluorescence peaks of the filter material are correctly eliminated. A slight minimum at the position of the Compton-band maximum results from the rigid and hence imperfect modelling of the inelastic part.

We therefore propose an improved algorithm. In each iteration only those inelastic contributions are eliminated that originate from non-dominating parts of the primary spectrum (in our case the fluorescence lines and the bremsstrahlung background are eliminated). This is done by subtraction of both the elastic and inelastic contributions of the dominating line as obtained by the least-squares modelling before the iteration:

$$I_1^{*(0)}(\omega_2) = I_2^*(\omega_2)\,, \tag{11}$$

$$I_1^{*(i+1)}(\omega_2) = I_2^*(\omega_2) - \int I_1^{*(i)}(\omega_1)\,A(\omega_1, \omega_2, \varphi) \cdot C(\omega_1, \omega_2, \varphi)\,J^{\mathrm{mod}}(q)\,\mathrm{d}\omega_1$$

with

$$I_2^*(\omega_2) = I_2(\omega_2) - I^{\mathrm{mod}}_{2,\,\mathrm{m}}(\omega_2)\,.$$

After convergence is reached (self-consistency of $I_1^*(\omega_1)$), the subtracted contributions are re-added. In this way only the inelastic contributions of the dominating AgKα_1 line are left. We then repeat the least-squares fit and obtain an improved model for the inelastic part.

The whole procedure therefore consists of two iterations, one within the other. The outer loop improves the model for the Compton profile successively, while the inner one removes all inelastic contributions of the non-dominating part of the primary spectrum on the basis of this model. Using this approach, the crudity of the original least-squares fit is overcome by subsequent refinement of the model until total self-consistency of both $J^{\mathrm{mod}}(q)$ and $I_1(\omega_1)$ is reached.

Figure 3c shows the result of this improved algorithm. All inelastic contributions in the scattering spectrum are eliminated, and the remaining spectrum consists of the dominating AgKα_1 line, the fluorescence lines of the filter materials and the rest of bremsstrahlung background. This is the true primary spectrum $I_1(\omega_1)$ seen by our target. A further important advantage over the direct measurement of the primary spectrum through attenuating slits or holes is the fact that the geometrical parameters are exactly the same as in the following Compton scattering measurements.

4. Conclusions

It is possible to correct the influences of polychromaticity in the primary radiation by the presented algorithms, which offers an improved evaluation of Compton scattering experiments with γ-radiation. It furthermore enables one to utilise sources of higher flux but lower degree of monochromatisation for Compton scattering experiments, e.g. the differentially filtered Ag radiation of a wide-focus tube. The "indirect" determination of an intense primary spectrum, on the other hand, is a general method, not restricted to the use of X-ray sources in Compton scattering experiments. It can be employed in all situations where intense γ- or X-ray sources are used and thus offers a wide field of applications.

[1] B. Williams (ed.), Compton Scattering. The Investigation of Electron Momentum Distributions, McGraw-Hill, New York 1977.
[2] M. J. Cooper, Rep. Prog. Phys. **48,** 415 (1985).
[3] G. Loupias and J. Petiau, J. Physique **41,** 265 (1980).
[4] N. Shiotani, N. Sakai, F. Itoh, M. Sakurai, H. Kawata, Y. Amemiya, and M. Ando, Nucl. Instrum. Methods Phys. Rev. **A 275,** 447 (1989).
[5] P. K. Bachmann, Dissertation, Darmstadt 1979.
[6] S. O. Manninen, M. J. Cooper, and D. A. Cardwell, Nucl. Instrum. Meth. Phys. Res. **A 245,** 485 (1966).
[7] A. J. Rollason, J. Felsteiner, G. E. W. Bauer, and J. R. Schneider, Nucl. Instrum. Meth. Phys. Res. **A 256,** 532 (1987).
[8] P. Eisenberger and W. A. Reed, Phys. Rev. B **9,** 3237 (1974).
[9] R. Ribberfors, Phys. Rev. B **12,** 2067 (1975).
[10] P. A. Ross, Phys. Rev. **28,** 425 (1926).
[11] M. R. Flannery and H. Levy, J. Chem. Phys. **50,** 2938 (1969).